Measurement 242 (2025) 115892

Contents lists available at ScienceDirect

Measurement

journal homepage: www.elsevier.com/locate/measurement

Detection of picometer scale vibration based on the microsphere near-field probe

Linzhi Yao [a,1], Yan Lu [a,1], Liyang Yue [b], Yunkai Wang [a], Zhicheng Cong [a], Yu Sun [a], Taiji Dong [a], Chunlei Jiang [a,*], Zengbo Wang [b,*]

[a] College of Electrical and Information Engineering, Northeast Petroleum University, Daqing 163318, China
[b] School of Computer Science and Electronic Engineering, Bangor University, Dean Street, Bangor, Gwynedd LL571UT, UK

ARTICLE INFO

Keywords:
Near field detection
Picometre vibration detection
Evanescent wave
Microsphere near-field probe

ABSTRACT

We introduce an innovative vibration detection method utilizing a microsphere near-field probe, affixed to an optical fiber probe. Notably, when the microsphere probe is positioned at a distance of approximately 100 nm from the vibrating objects, it exhibits a substantial increase in detection sensitivity, enabling the detection vibration as small as 5 pm. This enhancement arises from the strong near-field interaction between the sample and probe, where the evanescent wave dominates. This effect is confirmed for the first-time through both theoretical analysis and experimental validation. This innovative probe has great potential for applications in cellular acoustics, vibrational detection of biomolecules and their complexes, in situ measurements, and imaging of microstructures and nanostructures.

1. Introduction

Micro/nanoscopic biological entities, e.g. biomolecules, cells, and microorganisms, play an important role as the elemental constituents of living organisms[1]. Recently, there has been a growing interest in exploring the inherent vibrational dynamics of objects at mesoscopic scales[2]. This exploration extends to diverse functional particles[3,4], including a majority of biological cells and viruses[5]. The vibrational patterns exhibited by biological samples serve as valuable indicators of essential biomechanical properties, which can vary based on the species and environmental conditions. Consequently, the development of precise and sensitive biomedical detection techniques at the microscopic level becomes crucial for accurate disease prediction and effective treatment strategies. Especially, the development of atomic-scale detection methods is crucial as it enables ultra-high-resolution analysis, revealing intricate details of biomolecular and cellular processes. This advancement is instrumental in early disease diagnosis, precise drug design, and the understanding of complex biological systems. These methods offer unprecedented precision and detail, providing deeper insights into biological processes and holding immense potential for biomedical research and cellular diagnostics.

Moreover, employing near-field probes enables the non-contact detection of the structural and material properties of micro-objects. Based on this principle, scanning near-field optical microscopy (SNOM) was developed as a microscopy technique to overcome the far-field resolution limit by controlling evanescent waves for nanostructure characterization. The evanescent field generates around the target is created through a laser beam focused through an aperture smaller than the wavelength of the laser. Leveraging these features, SNOM can discover extremely small vertical movements on cell membranes within the range of 1 nm or less[6]. This capability allows real-time acquisition of structural information from molecules, ranging from individual molecules to larger entities. However, the miniaturization of nano-mechanical sensors remains challenging due to the inherent mechanism of mechanical feedback and active components used in SNOM. A compact vibration sensor holds potential compatibility with numerous detection applications, including intracellular, minimally invasive, and high-resolution detection[7].

In addition, the atomic force microscope (AFM), a type of scanning probe microscopy[8], employs a mechanical probe to 'touch' the material surface, achieving a resolution 1000 times better than the diffraction limit. This device can provide more accurate biological detection, e.g. measuring localized nanoscale vibrations from single-cell respiration[9,10], exploring intermolecular interactions between

* Corresponding authors.
E-mail addresses: jiangchunlei_nepu@163.com (C. Jiang), z.wang@bangor.ac.uk (Z. Wang).
[1] These authors contributed equally to this work.

https://doi.org/10.1016/j.measurement.2024.115892
Received 10 June 2024; Received in revised form 31 August 2024; Accepted 3 October 2024
Available online 9 October 2024

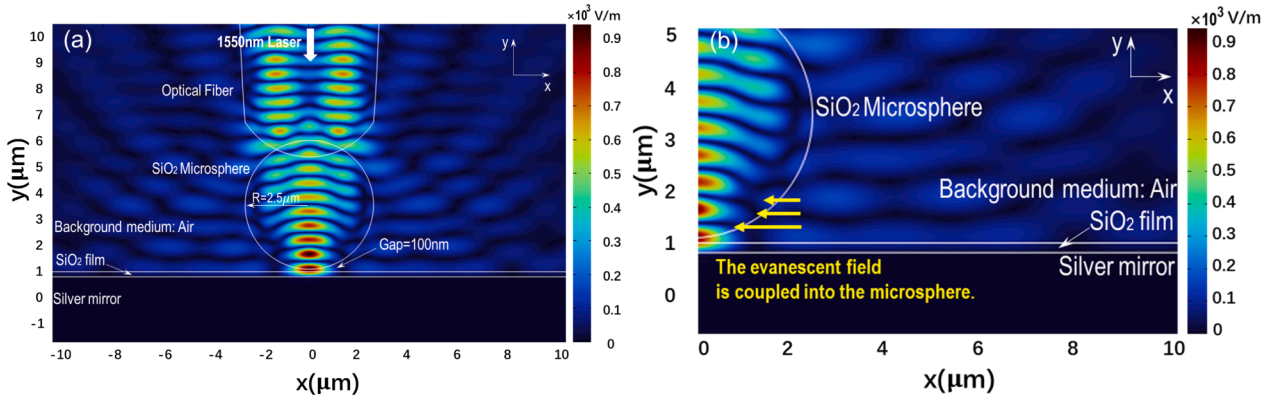

Fig. 1. (a) Incident light from the optical fiber excites the evanescent field on the surface of the object under measurement. (b) Evanescent wave coupling into probes microspheres.

receptors and ligands in biological systems, and examining the mechanics of individual living cells and biomolecules[11,12]. Nevertheless, when AFM operates in contact mode, it is noted that the contact and interaction between the AFM tip and the object surface introduce errors and unnecessary displacements in detection[13,14]. Moreover, when dealing with live cells as the measurement target, the movement of the AFM cantilever and SNOM laser may penetrate or damage the cell membranes during vibration detection[15,16], resulting in irreversible damage to cell structures, rupture of some cellular organisms, and loss of biological information. For AFM operating in non-contact modes such as tapping mode, the probe gently "taps" on the cell surface rather than maintaining continuous contact. The brief interactions between the probe and the cell generate a series of detectable force signals. This method of detecting cell vibrations significantly reduces the risk of cell damage. However, to ensure optimal detection results, precise control of frequency and amplitude is required, and the slow detection speed adds considerable difficulty to the process. Additionally, the AFM cantilever and the apertured probe of SNOM are delicate core components for the mentioned detections, used as expensive consumables that add complexity and difficulty to experiments [17]. Consequently, repeating measurements would be slow and high-cost and possess a higher risk of damaging the entire biological system in the experiment. Currently, the detection resolution of vibration of biological samples is still at the micrometer and nanometer level. However, nanoscale vibration detection is not sufficient for probing the biomechanical properties of cells and intracellular signaling. Therefore, there is an urgent need for a new method to achieve picometer level cell vibration detection.

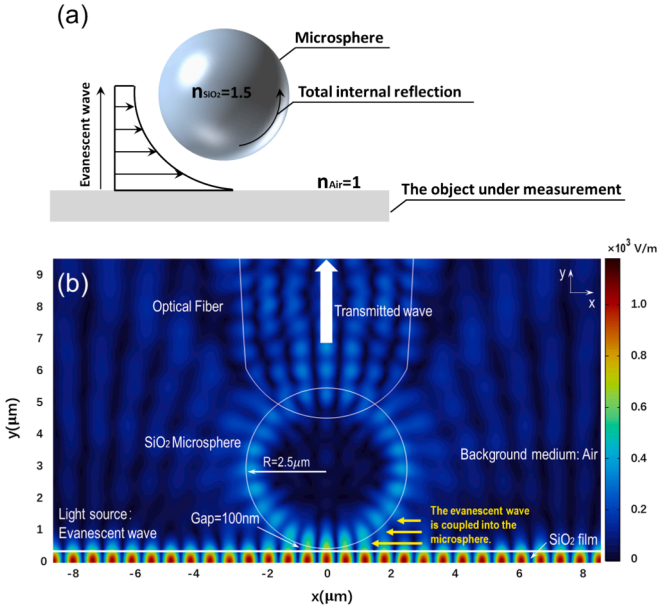

Fig. 2. (a) Schematic of the evanescent wave coupling into the microsphere. (b) Schematic of the fiber optic probe collecting the evanescent wave from the surface of the object under measurement.

Traditional optical detection can also achieve nanoscale and sub-nanoscale micro-vibration detection. Zhang et al.[18] pioneered an all-fiber aberration detection system, featuring an all-fiber acousto-optic design. This innovation achieved a remarkable minimum detected vibration amplitude of 6 pm. Shang et al.[19] further advanced the field by introducing a high spatial-resolution all-fiber laser Doppler vibrometer, offering an impressive displacement resolution of 2.5 pm for aberration detection. Lipiäinen et al. [20] proposed a novel method employing laser-based aberration interferometry to detect vibration phase and absolute amplitude with a precision of approximately 1 pm. In contrast to the near-field scanning approaches, the aforementioned optical detection relying on aberration interferometers often requires a sophisticated modulation/demodulation system to attain sub-nanometer vibration detection. The related disadvantages include high power consumption of the light source, intricate system structures, and a relatively high cost, causing optical detections less practical for applications involving the detection of microscopic biological objects and biological macromolecules.

With the evolution of fiber optic technology, microsphere probe sensors boasting a straightforward structure and superior resolution find extensive application in temperature[21], displacement and vibration detection[22–24]. Nevertheless, the resolution of existing microsphere probe sensors remains constrained to the nanometer and sub-nanometer levels. This limitation proves challenging as it fails to satisfy the high-precision demands necessary for accurately detecting biological vibrations.

To address the demand for precise vibration detection for biological cells, we developed an innovative method that employs a microsphere near-field probe positioned within 100 nm of the object surface. This approach can generate the robust evanescent near-field interaction between the sample and the probe, presenting exceptional detection sensitivity with an impressive accuracy down to 5 pm. Notably, this method boasts the merits of being non-contact, possessing high resolution, and featuring a straightforward structure. Its advantages position it as a promising technology for various applications, including cellular acoustics, biomolecular vibration detection, and imaging of micro- and nanostructures.

2. Theory and experiments design

As illustrated in Fig. 1, The incident light from the optical fiber is reflected by the substrate and experiences total internal reflection (TIR)

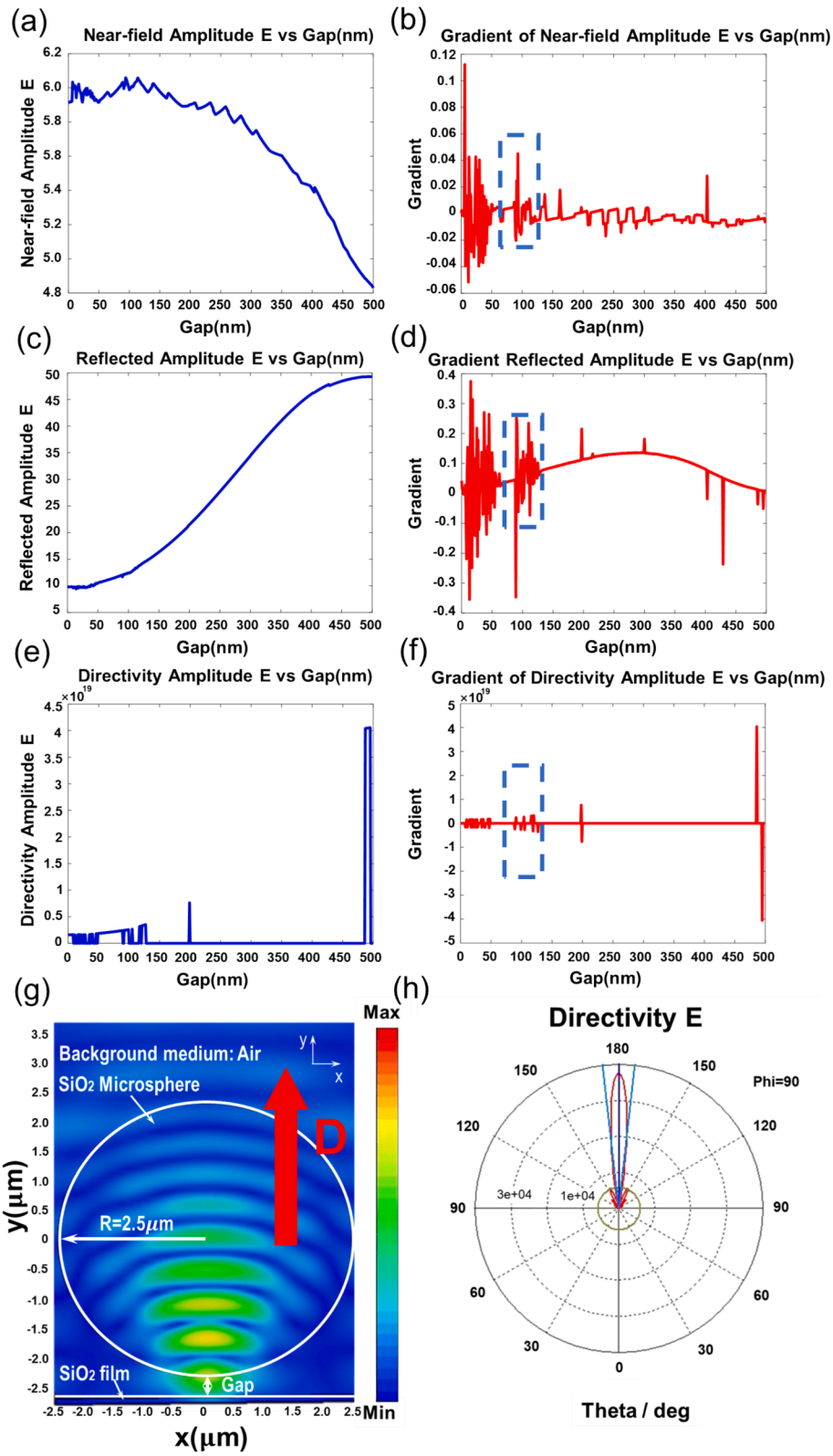

Fig. 3. (a) Near-field intensity. (b) Near-field intensity change rate. (c) Reflected-beam intensity. (d) Reflected-beam intensity change rate. (e) Scattering directivity and direction. (f) Scattering directivity change rate. (g) Light field distribution of microsphere probes. (h) Light field distribution in polar coordinates with significantly enhanced scattering in the direction of probe acquisition.

on the internal surface of the object being measured. while TIR occurs, the energy of the incident light is not wholly reflected at a specific plane but instead gradually reflected after penetrating to a specific depth into the medium (air). This results in the generation of evanescent waves on the surface of the object under measurement.

In order to simulate the microsphere probe excitation of evanescent waves on the surface of the object being measured in the near field, we utilize Comsol Multiphysics 6.1 to simulate the model. We utilized the

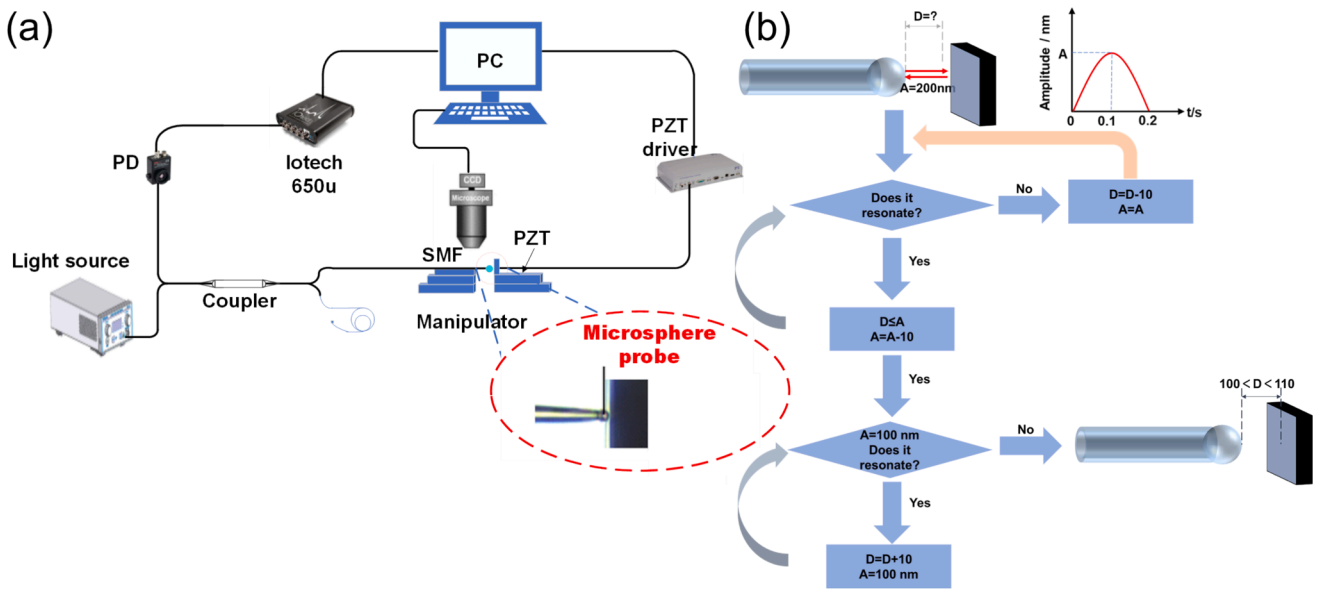

Fig. 4. (a) Diagram of the Experimental Setup. (b) Flow chart for controlling the distance between probe and PZT to be about 100 nm.

Wave Optics Module (Electromagnetic Waves, Frequency Domain) in the software and applied Perfectly Matched Layer (PML) boundary conditions for the two-dimensional simulation. The electric field intensity distribution was analyzed using boundary mode analysis. We simulated the microsphere probe with a fiber tip diameter of 6 μm and a microsphere diameter of 5 μm. In this work, the substrate of the object being measured is silver, with a SiO_2 thin film on the surface. The axis of the microsphere probe is set at x = 0, and the tip position of the microsphere is at x = 0 μm, y = 1.1 μm. The microsphere probe is spaced 100 nm away from the SiO_2 thin film surface. The background medium in the model is air, with a refractive index of 1. The refractive indices of the optical fiber, the SiO_2 microsphere, and the SiO_2 thin film are all 1.5. The light source is injected into the fiber, and the wavelength of the incident is 1550 nm. Since it was not possible to measure the input power at the port during the simulation, a normalization approach was employed, we set the input power to 1 mW.

The evanescent wave coupling from the object's surface enters the microsphere, where the light is restricted within the microsphere cavity due to continuous TIR, as depicted in Fig. 2(a).

Following Snell's law, the intensity of the evanescent field can be expressed as:

$$E_t = E_{0t} e^{-i(\omega t - x k_t \sin\theta n)} e^{-nzk_t \sqrt{\sin^2\theta - (1/n)^2}} \tag{1}$$

Its depth of penetration is:

$$z_0 = \frac{\lambda/n}{2\pi\sqrt{\sin^2\theta - (1/n)^2}} \tag{2}$$

where n is the refractive indices of the object to be measured,θ is the angle of incidence,E_t is the intensity of the evanescent field,E_{0t} is the initial intensity (constant),k_t is the propagation factor.

According to equations (1) and (2), it is evident that the evanescent wave excited on the surface of the measured object decreases exponentially in intensity along the z-direction. When the $\Delta z \ll z_0$, the change in the intensity of the evanescent field E_t has a good linear relationship with the change in the amplitude of the measured object Δz:

$$E_t \approx \alpha \Delta z \tag{3}$$

where α is the scale factor, a constant.

We present an innovative fiber-optic probe that combines optical fiber and microsphere components. When the refractive indices of the optical fiber and the microsphere match, light can be transmitted between them without any obstruction. We utilized Comsol Multiphysics 6.1 to perform equivalent simulations on the ability of the microsphere probe to couple near-field evanescent waves and convert them into far-field transmitted waves. A transverse light field is incident into the surface of the object being measured, which is equivalent to a standing wave on the surface of the object, and is collected using the microsphere probe, as shown in Fig. 2(b). We utilized the Wave Optics Module (Electromagnetic Waves, Frequency Domain) in the software and applied Perfectly Matched Layer (PML) boundary conditions for the two-dimensional simulation. The electric field intensity distribution was analyzed using boundary mode analysis. We simulated the microsphere probe with a fiber tip diameter of 6 μm and a microsphere diameter of 5 μm. In this model, the background medium is air with a refractive index of 1. The refractive indices of the optical fiber, the SiO_2 microsphere, and the SiO_2 thin film are all 1.5. The light source is an evanescent wave that propagates along the surface of the SiO_2 thin film, and the wavelength of the incident is 1550 nm. Since it was not possible to measure the input power at the port during the simulation, a normalization approach was employed, we set the input power to 1 mW.

From the simulation, we can know that the microspheres effectively converting the evanescent wave signal from the object's surface into a transmitted wave signal. This improvement significantly enhances the precision and sensitivity of the detecting technique.

We utilized the commercial simulation software CST Studio, an electromagnetic full-wave simulator based on the Finite Integral Technique (FIT) method, to simulate the detection sensitivity of a 5 μm microsphere probe with a refractive index of 1.5. This involved simulating and predicting near-field intensity, reflected-beam intensity, and scattering Directivity (D) across the gap distance between the sample and the probe (ranging from 0 nm to 500 nm) against the field intensity (amplitude E), as illustrated in Fig. 3. The probe sensitivities, represented by the gradients of the functions in Fig. 3 (a, c, and e), are demonstrated in Fig. 3 (b, d, and f). It is noted that a strong near-field interaction appears when the probe is positioned at 100 nm (within the blue dotted box in Fig. 3) from the object, resulting in significant increases in detection sensitivity.

In this case, the Near-field intensity refers to the transverse standing wave intensity on the surface of the measured object, specifically the electromagnetic field intensity near the object's surface. Reflected beam intensity refers to the strength of the return light signal collected back inside the probe. The scattering directivity (D) of the electric field

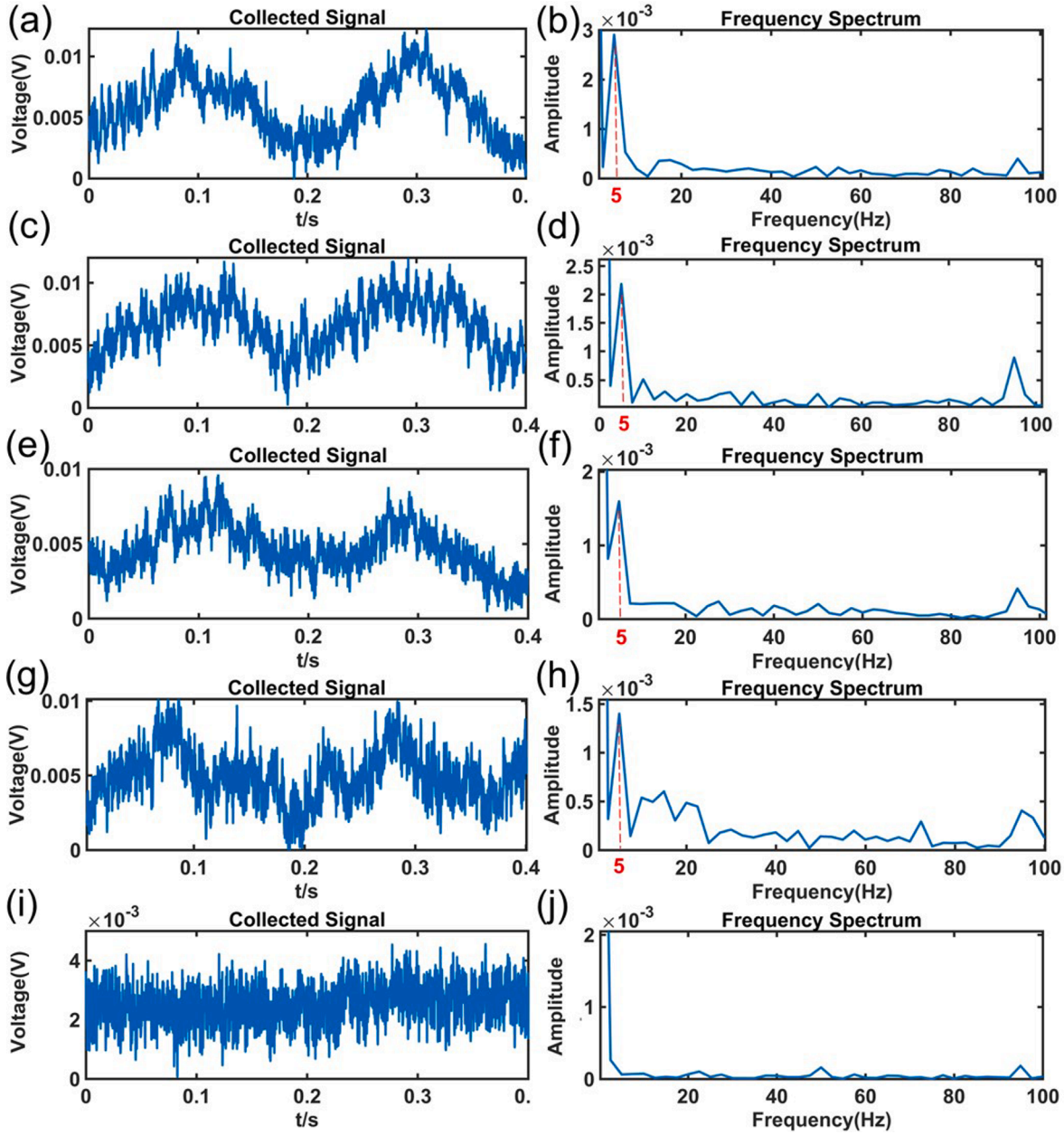

Fig. 5. Sub-nanometer vibration detection signal diagram. (a) 1 nm Vibration Signal. (b) 1 nm Frequency Signal. (c) 800 pm Vibration Signal. (d) 800 pm Frequency Signal. (e) 600 pm Vibration Signal. (f) 600 pm Frequency Signal. (g) 400 pm Vibration Signal. (h) 400 pm Vibration Signal. (i) Probe and the object at a distance of 350 nm, 400 pm Vibration Signal. (j) Probe and the object at a distance of 350 nm, 400 pm Frequency Signal.

intensity indicates the degree to which the electromagnetic field radiates electromagnetic waves in a specific direction (D). The near-field intensity change rate refers to the rate at which the electromagnetic field intensity changes with respect to its spatial position in the y-direction within the near-field range. The reflected-beam intensity change rate refers to the rate at which the strength of the return light signal collected back inside the probe changes with respect to its spatial position in the y-direction. Finally, the scattering directivity change rate refers to the rate at which the degree of radiation of light in direction D changes with respect to its spatial position in the y-direction.

The experimental setup was designed in accordance with the simulation results. A single-mode optical fiber with a cladding diameter of 125 μm and a core diameter of 9 μm was employed to create a tapered fiber tip attaching the sphere probe using the hot-melt stretching method. The facet end of the fiber was pulled to form a uniform taper with a width of 5 μm. The wider fiber tip can ensure the rigidity of the fiber and increase the contact area for the microsphere probes to be attached, meanwhile significantly reducing light loss and contributing to measurement stability. A SiO_2 microsphere, with a diameter of 5 μm and a refractive index of 1.50, was bonded to the tapered fiber tip using ultraviolet (UV)–cured epoxy resin to create a complete microsphere probe.

The overall experimental configuration, shown in Fig. 4(a), featured a distributed feedback laser (DFB) with a wavelength of 1550 nm (Thorlabs, S1FC1550) as the light source. Laser light entered the fiber optic probe through a 2 × 2 coupler (TN1550R5A2). As the piezoelectric ceramic displacement table (PZT) induced vibrations, the vibration information of the object captured by the probe was transmitted to the photodetector (PD) via an optical fiber. Subsequently, the signals after analog-to-digital conversion were processed by a PC equipped with a data acquisition card (IO tech).

In line with the simulation results, the piezoelectric displacement

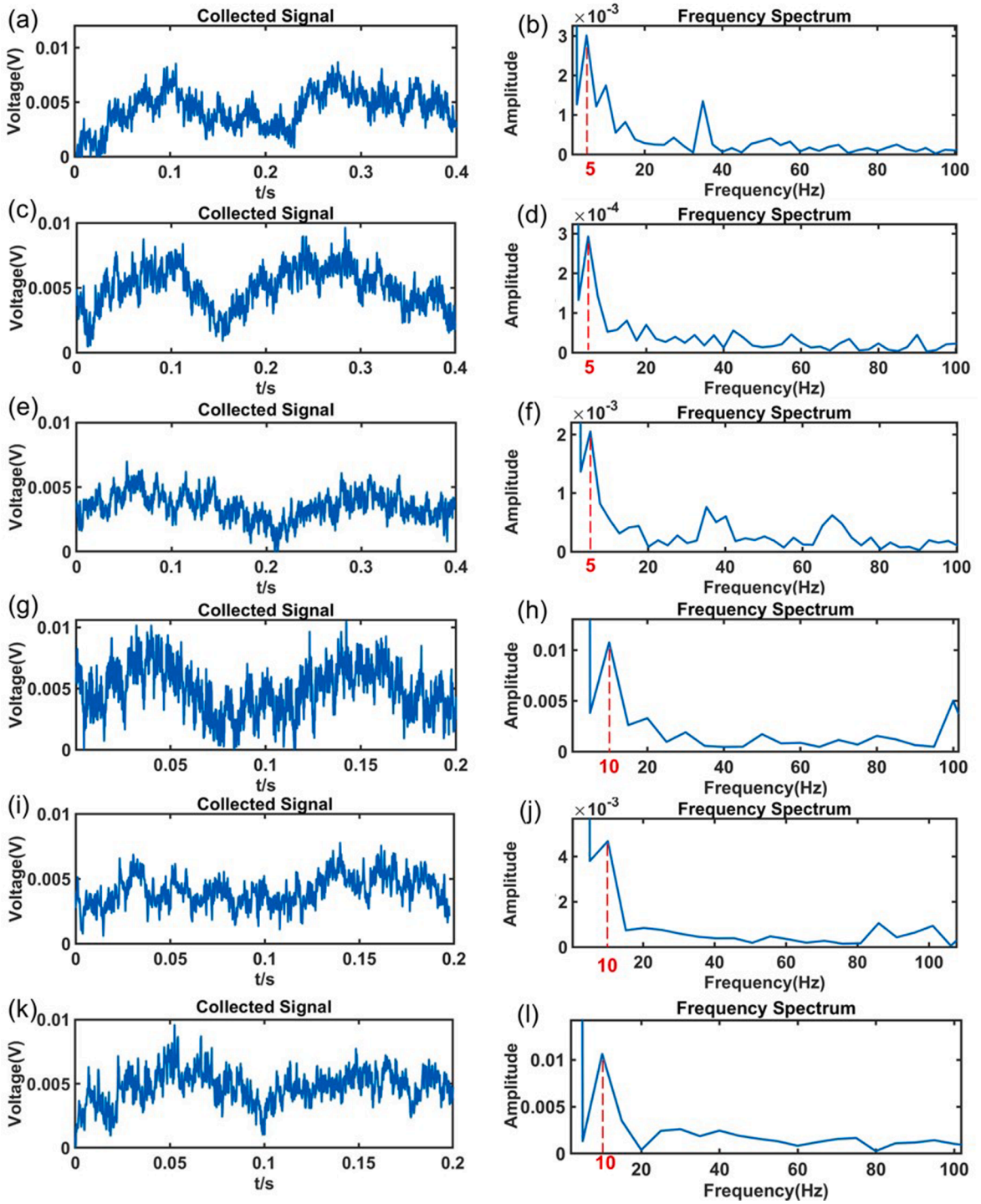

Fig. 6. Picometer vibration detection signal diagram. (a) 20 pm Vibration Signal. (b) 20 pm 5 Hz Frequency Signal. (c) 10 pm Vibration Signal. (d) 10 pm 5 Hz Frequency Signal. (e) 5 pm Vibration Signal. (f) 5 pm 5 Hz Frequency Signal. (g) 20 pm Vibration Signal. (h) 20 pm 10 Hz Frequency Signal. (i) 10 pm Vibration Signal. (j) 10 pm 10 Hz Frequency Signal. (k) 5 pm Vibration Signal. (l) 5 pm 10 Hz Frequency Signal.

stage maintained a consistent distance of 100 nm between the object and the microsphere probe to realize the best detection sensitivity. We controlled the distance between the probe and the PZT to 100 nm by vibrating the PZT and observing whether the probe resonated with it. Where D is the distance between the probe and the PZT and A is the amplitude of the PZT. "+" means the PZT is stepping closer to the probe, and "-" means the PZT is stepping away from the probe, this process is shown in Fig. 4(b).

3. Results

Sub-nanometer vibrations were induced by a piezoelectric transducer (PZT) driven by a sinusoidal signal at frequencies of 5 Hz and amplitudes of 1 nm, 800 pm, 600 pm, and 400 pm, respectively. The experimental results illustrating the detected signals and corresponding frequencies are illustrated in Fig. 5 for the aforementioned vibration amplitudes. These results highlight the capability of the current setup, relying on the microsphere probes, to accurately detect all picometer-

scale vibrations. In contrast, when the distance between the probe and the measured object was increased, e.g., to 350 nm, as demonstrated in Fig. 5 (i and j), the 400 pm vibration signal became completely submerged in noise, resulting in a failed detection. When the amplitudes were further reduced to 20 pm, 10 pm, and 5 pm with the frequency of 5 Hz, the proposed approach still accomplished the vibration detection, as shown in Fig. 6(a)-(f). Additionally, to verify the reliability and repeatability of the detection, the vibrations with the frequency of 10 Hz and the same amplitudes of 20 pm, 10 pm, and 5 pm were measured using the current setup. The corresponding detection results are shown in Fig. 6 (g)-(l) and in accordance with the vibration features of PZT.

All experimental results demonstrate the outstanding performance of the proposed system in detecting picometer-scale vibrations, achieving a measurement limit of 5-pm amplitude. As a key experimental indicator, the minimum measurable vibration is significantly influenced by noise from the light source, laser quantum fluctuations, and background interference. To enhance measurement accuracy and mitigate noise interference, the laser light source was carefully enclosed using acoustic cotton wool. Furthermore, the entire system was installed on an optical table within a temperature-controlled laboratory environment, effectively minimizing the impact of external factors such as temperature variations, airflow, and structural vibrations.

4. Conclusion

In conclusion, we invented a picometer-scale vibration detection system leveraging an innovative microsphere near-field probe. By situating the microsphere probe approximately 100 nm from vibrating objects, a strong near-field evanescent-wave interaction emerging between the sample and the probe significantly improved the detection sensitivity. This enhancement enables the detection of vibrations as small as a 5-picometer displacement. The system shows promising potential for detecting nanometer and sub-nanometer vibrations in a wide range of biological samples. Its advantages include non-contact operation, structural simplicity, high sensitivity, and in-situ detection capabilities, making it applicable in multiple areas, such as cellular acoustics, biomacromolecular and complex vibration detection, micro- and nanostructural imaging, as well as in-situ measurements.

Funding

Chunhui Plan of the Ministry of Education (HZKY20220304); Leverhulme Trust Fellowship (RF-2022-659); Royal Society (IEC\R2 \202178).

CRediT authorship contribution statement

Linzhi Yao: Writing – review & editing, Writing – original draft, Visualization, Software, Methodology, Investigation, Formal analysis, Data curation. **Yan Lu:** Writing – review & editing, Writing – original draft, Software, Methodology, Investigation, Formal analysis, Data curation. **Liyang Yue:** Writing – review & editing, Supervision, Methodology, Conceptualization. **Yunkai Wang:** Software, Data curation. **Zhicheng Cong:** Software, Methodology, Data curation, Conceptualization. **Yu Sun:** Supervision, Methodology, Conceptualization. **Taiji Dong:** Resources, Data curation, Conceptualization. **Chunlei Jiang:** Supervision, Methodology, Funding acquisition, Conceptualization. **Zengbo Wang:** Supervision, Software, Methodology, Investigation, Formal analysis, Data curation, Conceptualization.

Declaration of competing interest

The authors declare that they have no known competing financial interests or personal relationships that could have appeared to influence the work reported in this paper.

Data availability

Data underlying the results presented in this paper are not publicly available at this time but may be obtained from the authors upon reasonable request.

Acknowledgments

This work was supported by the Chunhui Plan of the Ministry of Education, China (HZKY20220304), the Leverhulme Trust Fellowship, UK (RF-2022-659) and the Royal Society, UK (IEC\R2\202178).

References

[1] X. Hu, et al., Review on near-field detection technology in the biomedical field, Adv. Photon. Nexus 2 (2023).
[2] S.-J. Tang, et al., Single-particle photoacoustic vibrational spectroscopy using optical microresonators, Nat. Photonics 17 (2023) 951–956.
[3] R.C. LeCraw, et al., Extremely low loss acoustic resonance in single-crystal garnet spheres, Phys. Rev. Lett. 6 (1961) 620.
[4] X. Zhang, et al., Cavity magnomechanics, Sci. Adv. 2, e1501286.
[5] M. Tayebi, et al., Massively multiplexed submicron particle patterning in acoustically driven oscillating nanocavities, Small 16 (2020).
[6] R. Piga, et al., Acoustical nanometre-scale vibrations of live cells detected by a near-field optical setup, Opt. Express 15 (2007) 5589–5594.
[7] Y. Shi, et al., Nanoscale fiber-optic force sensors for mechanical probing at the molecular and cellular level, Nat. Protoc. 13 (2018) 2714–2739.
[8] Y. Tian, et al., Development of a XYZ scanner for home-made atomic force microscope based on FPAA control, Mech. Syst. Sig. Process. 131 (2019) 222–242.
[9] R. Garcia, Nanomechanical mapping of soft materials with the atomic force microscope: methods, theory and applications, Chem. Soc. Rev. 49 (2020) 5850–5884.
[10] S. Hsieh, et al., Advances in cellular nanoscale force detection and manipulation, Arab. J. Chem. 12 (2019) 3163–3171.
[11] F.S. Ruggeri, et al., Atomic force microscopy for single molecule characterisation of protein aggregation, Arch. Biochem. Biophys. 664 (2019) 134–148.
[12] T. Kwon, et al., Atomic force microscopy-based cancer diagnosis by detecting cancer-specific biomolecules and cells, Biochimica et Biophysica Acta (BBA) - Reviews on Cancer 1871 (2019) 367–378.
[13] L. Venturelli, et al., A perspective view on the nanomotion detection of living organisms and its features, J. Mol. Recognit. 33 (2020) e2849.
[14] B. Zhang, et al., Imaging and analyzing the elasticity of vascular smooth muscle cells by atomic force acoustic microscope, Ultrasound Med. Biol. 38 (2012) 1383–1390.
[15] S. Ryu, et al., Nanoneedle insertion into the cell nucleus does not induce double-strand breaks in chromosomal DNA, J. Biosci. Bioeng. 116 (2013) 391–396.
[16] S.-W. Han, et al., Evaluation of the insertion efficiencies of tapered silicon nanoneedles and invasiveness of diamond nanoneedles in manipulations of living single cells, Arch. Histol. Cytol. 72 (2009) 261–270.
[17] Q. Lyu, et al., Double-peak resonant mapping of cellular viscoelasticity in force-clamp detection of atomic force microscope, J. Sound Vib. 527 (2022) 116869.
[18] W. Zhang, et al., Optical heterodyne micro-vibration measurement based on all-fiber acousto-optic frequency shifter, Opt. Express 23 (2015) 17576–17583.
[19] J. Shang, et al., Experimental study on minimum resolvable velocity for heterodyne laser Doppler vibRometry, Chin. Opt. Lett. 9 (2011) 081201.
[20] L. Lipiäinen, et al., Phase sensitive absolute amplitude detection of surface vibrations using homodyne interferometry without active stabilization, J. Appl. Phys. 108 (2010) 114510.
[21] H.B. Chen, et al., A miniature fiber tip polystyrene microsphere temperature sensor with high sensitivity, Photonic Sensors 12 (2022) 84–90.
[22] P. Robalinho, O. Frazao, Nano-displacement measurement using an optical drop-shaped structure, IEEE Photon. Technol. Lett. 33 (2021) 65–68.
[23] K. Tian, et al., Miniature Fabry-Perot interferometer based on a movable microsphere reflector, Opt. Lett. 45 (2020) 787–790.
[24] Y. Yang, et al., Ultrahigh-sensitivity displacement sensing enabled by the Vernier effect with inhibited antiresonance, Opt. Lett. 46 (2021) 1053–1056.